Laser Physics Letters

Astro Ltd.

LETTER

Controlling multiple diffraction with quasiperiodic gratings

To cite this article: D A Ikonnikov *et al* 2019 *Laser Phys. Lett.* **16** 126202

IOP Publishing | Astro Ltd
Laser Physics Letters
Laser Phys. Lett. **16** (2019) 126202 (5pp)
https://doi.org/10.1088/1612-202X/ab5845

Letter

Controlling multiple diffraction with quasiperiodic gratings

D A Ikonnikov[1], V G Arkhipkin[1,2] and A M Vyunishev[1,2]

[1] Kirensky Institute of Physics, Federal Research Center KSC SB RAS, Krasnoyarsk, 660036, Russia
[2] Department of Photonics and Laser Technology, Siberian Federal University, Krasnoyarsk, 660079, Russia

E-mail: vyunishev@iph.krasn.ru

Received 7 October 2019
Accepted for publication 8 November 2019
Published 2 December 2019

Abstract

Complex diffraction patterns are formed by sophisticated diffraction gratings. However, the methods of synthesizing of such gratings are complicated and resource intensive. We propose a simple analytical approach to forming one- and two-dimensional quasiperiodic gratings supporting multiple diffraction consisting of a set of diffraction maxima with the specified spatial frequency of certain diffraction order. The structure of a quasiperiodic grating is a superposition of harmonic functions, which provide a discrete spatial spectrum. The number of diffraction maxima, their angular positions, and intensity distribution between them can be controlled by choosing appropriate reciprocal lattice vectors and their amplitudes. This effect confirmed by the experiment opens new possibilities for light shaping, imaging, and radiation coupling.

Keywords: diffraction gratings, multiple diffraction, quasiperiodic gratings

(Some figures may appear in colour only in the online journal)

1. Introduction

A diffraction grating (DG) is an optical component with a periodic structure that splits and diffracts light into several beams propagating in different directions, depending on the grating period, light wavelength, and angle of incidence. The gratings are commonly used to separate light into wavelength components and have a wide application range spanning from spectroscopy and laser technologies to probing of single molecules in biological samples [1]. The generalized DGs can be used to obtain different numbers of diffraction orders with equal [2] and tailored intensity [3], as well as to suppress the high-order diffraction [4]. In recent years, aperiodic and quasiperiodic structures have aroused interest in the optical community. The linearly chirped gratings made it possible to control the angular width of diffraction orders, which can be used to ensure uniform illumination over a specified angular range [5]. It was demonstrated that quasiperiodic gratings can produce diffraction orders propagating along curved trajectories [6]. Fibonacci gratings can keep the imaging characteristics intact even if significant loss of information occurs due to their redundancy and robustness [7]. In addition, they are used to transform evanescent waves into propagating ones for far-field super-resolution imaging [8]. Thue–Morse [9] and Fractal [10] diffraction optical elements exhibit the fascinating focusing and self-similarity properties.

There exists a multifunctional method for constructing the desired optical wavefront with the use of objects numerically specified by computer-generated holograms [11, 12] also known as array illuminators [13, 14]; this requires, however, intricate computations and makes the procedure of hologram reconstruction unapparent. Recently, this method has been extended to the generation of nonlinear optical holograms [15, 16].

For some purposes, like beam splitting or coupling, it is not necessary to make full Fourier transform and calculate

respective coefficients. It is more convenient to elaborate a simple and undemanding way to obtain arbitrary diffraction patterns with finite number of maxima in each order with specified angular positions. For this, the Raman–Nath diffraction can be used, but an appropriate diffraction pattern will have a single maximum for each diffraction order, which occurs at the fixed angular interval [17]. A fairly simple analytical method proposed recently to produce quasiperiodic structures with a discrete spatial spectrum is called the superposition method. In nonlinear optics, it is considered promising for the multi-wavelength conversion [18–21] and multiple spatial harmonic generation [22]. In addition, this method was used to produce a structure of one-dimensional photonic crystals with adjustable multiple photonic band gaps [23]. Therefore, the superposition method is promising for structuring quasiperiodic diffraction gratings (QPDGs), which produce arbitrary diffraction patterns.

In this letter, we propose a straightforward way for composing quasiperiodic DGs with predefined multiple beams for each diffraction orders via a superposition of several phase sublattices with different periods. We show that the diffraction pattern of such QPDGs is a set of diffraction patterns of individual periodic DGs.

2. Theoretical model

The complex modulation function of an arbitrary one-dimensional DG is

$$t(x) = T(x)e^{-i\Phi(x)}, \tag{1}$$

where $T(x)$ is the amplitude modulation function and $\Phi(x)$ is the phase modulation function.

We will focus on the phase modulation, assuming $T(x) = \text{const}$ in (1). The phase modulation function of the proposed binary one-dimensional QPDG can be described as

$$\Phi(x) = \Phi_0 + \Delta\Phi \cdot \text{sgn}(\sum a_n \cos[G_n x + \phi_n]). \tag{2}$$

Here, Φ_0 is the average phase, $\Delta\Phi$ is the maximum deviation of the phase from its average value Φ_0, a_n, and ϕ_n are the amplitude and relative phase of the nth spatial harmonic, $\text{sgn}(\psi) = |\psi|/\psi$ is the signum function of the argument ψ, $G_n = |\mathbf{G}_n| = 2\pi/\Lambda_n$ is the absolute value of the reciprocal lattice vector (RLV), and Λ_n is the period of $\cos(G_n x)$ function. We limit the consideration to the case of two elements in the sum, assuming $\phi_{1,2} = 0$, so that (2) takes the form

$$\Phi(x) = \Phi_0 + \Delta\Phi \cdot \text{sgn}\,(a_1 \cos G_1 x + a_2 \cos G_2 x)\,. \tag{3}$$

The phase modulation becomes periodic if any of the two amplitudes in (3) is zero.

According to the Fresnel–Kirchhoff diffraction equation, the electric field in a diffraction pattern at the point $\{x, y, z\}$ is given by

$$U(x, y, z) = \frac{1}{i\lambda} \int \int_{-\infty}^{\infty} U(x_0, y_0, 0) \frac{e^{ik\rho}}{\rho} dx_0 dy_0. \tag{4}$$

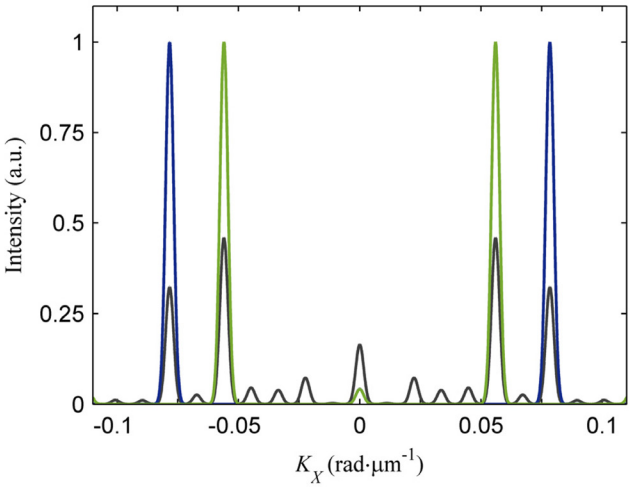

Figure 1. Calculated intensity distributions for the periodic DGs with $G_1 = 0.0785$ rad $\cdot$ μm^{-1} (blue) and $G_2 = 0.0561$ rad $\cdot$ μm^{-1} (green) and the quasiperiodic DG (black). The spatial frequency scale is $K_X = 2\pi x/(\lambda z)$.

Here, $k = 2\pi/\lambda$ is the wavevector and $\rho = \sqrt{(x - x_0)^2 + (y - y_0)^2 + z^2}$ is the distance between coordinates in the object $\{x_0, y_0\}$ and image $\{x, y\}$ planes.

In the calculation of the far-field diffraction patterns, (4) is used ($I(x,y,z) = 1/2|U(x,y,z)|^2$). Keeping both terms in (3), we obtain the spatial modulation of the phase corresponding to the QPDG structure. In the calculation, we used the same parameters as in the experiment described below, specifically, $\Phi_0 = \pi/2$, $\Delta\Phi = \pi/2$, $a_1 = a_2 = 1$, $G_1 = 0.0785$ rad $\cdot$ μm^{-1} ($\Lambda_1 = 80$ μm), and $G_2 = 0.0561$ rad $\cdot$ μm^{-1} ($\Lambda_2 = 112$ μm). The angular distribution of the intensity of light diffracted on the structure described by (3) has two peaks in the far-field, which correspond to the spatial frequencies $\pm G_1$ and $\pm G_2$ (figure 1(black)) instead of the solitary maxima for the periodic DGs with the main reciprocal lattice vectors $\pm G_1$ (blue) and $\pm G_2$ (green), respectively. Since the number of maxima in the diffraction pattern of a quasiperiodic DG is greater than in the case of a periodic DG, the total intensity is distributed over the larger number of components and the intensity of individual maxima in the QPDG weakens.

We expect that the amplitude values a_n would control the intensity distribution between diffraction maxima [21]. For confirmation we made calculations of intensity distributions for quasiperiodic DGs with different amplitude values a_n, assuming that $a_1^2 + a_2^2 = 1$ (figure 2). In the marginal cases ($a_1^2 = 1$, $a_2^2 = 0$ and $a_1^2 = 0$, $a_2^2 = 1$), the diffraction grating becomes periodic and has single maximum at corresponding spatial frequency. At the intermediate case ($a_1^2 \neq 0$ and $a_2^2 \neq 0$), the grating is quasiperiodic with the set of diffraction maxima at the specified spatial frequency of certain diffraction order. The distribution of intensities of the maxima depends on ratio between a_1 and a_2.

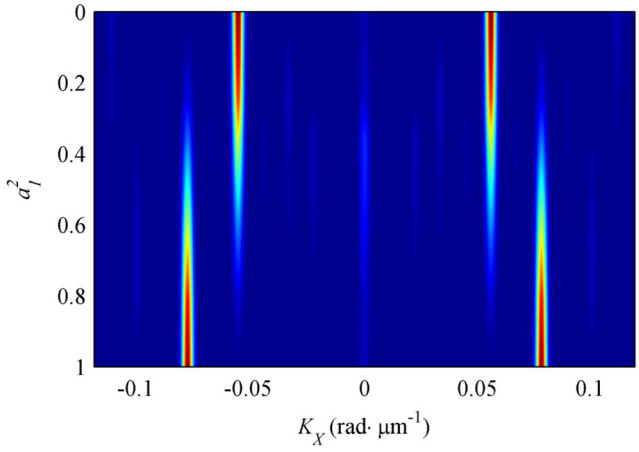

Figure 2. Calculated intensity distribution on the amplitude value a_1^2 ($a_1^2 + a_2^2 = 1$) for the quasiperiodic DGs with $G_1 = 0.0785$ rad· μm^{-1} and $G_2 = 0.0561$ rad · μm^{-1}. The spatial frequency scale is $K_X = 2\pi x/(\lambda z)$.

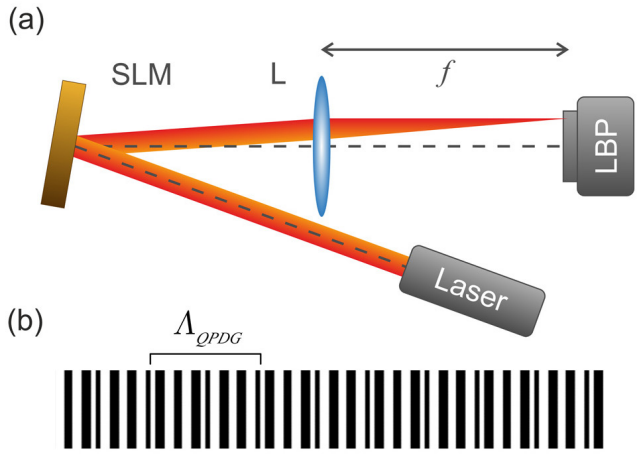

Figure 3. (a) Schematic of the experimental setup: spatial light modulator SLM, lens L, and laser beam profiler LBP. (b) Part of the binary one-dimensional phase modulation of a quasiperiodic DG.

3. Results and discussion

Figure 3(a) shows an experimental setup for the proof-of-concept experiments. The QPDG binary phase modulation pattern is calculated using (3) and loaded onto a 2D phase-only spatial light modulator (SLM, PLUTO-NIR-011, Holoeye, the spatial resolution is 1920 × 1080 pixels, and the pixel pitch is 8 μm). A part of the quasiperiodic DG phase modulation function is presented in figure 3(b). The SLM active area is illuminated by the linearly polarized radiation from He–Ne laser ($\lambda = 632.8$ nm) incident at an angle of 7.5 deg. The diffraction pattern is projected by a lens with $f = 10$ cm onto a laser beam profiler (LBP-1, Newport, pixel sizes 9.05 × 8.3 μm^2).

At $a_1 = a_2$, the cosine sum in (3) can be expressed as the cosine multiplication; therefore, the quasiperiodic function can be presented as a modulation of the low-frequency periodic function ($\cos(G_l) = \cos([G_1 - G_2]/2)$) by the high-frequency periodic function ($\cos(G_h) = \cos([G_1 + G_2]/2)$). Since the QPDG pattern is loaded onto the SLM with a finite pixel size, we have to choose such G_1 and G_2 values so all the layers in the structure were even integers of the SLM pixel size and the ratio G_h/G_l was a rational number (under the condition $\phi_1 = \phi_2$). The highest common factor of G_1 and G_2 is a reciprocal lattice vector corresponding to the quasiperiodic DG period $\Lambda_{QPDG} = 560$ μm. It was found that the values of $G_1 = 0.0785$ rad · μm^{-1} (a) and $G_2 = 0.0561$ rad· μm^{-1} satisfy this experimental criterion.

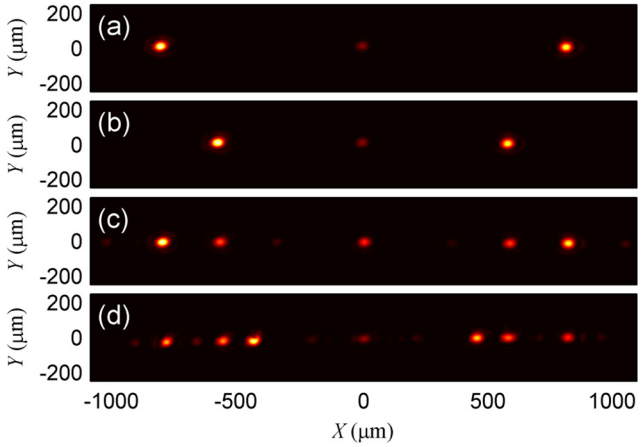

Figure 4. Experimental diffraction pattern for a periodic DG with (a) $\Lambda_1 = 80$ μm ($G_1 = 0.0785$ rad· μm^{-1}) and (b) $\Lambda_2 = 112$ μm ($G_2 = 0.0561$ rad· μm^{-1}) and (c) a quasiperiodic DG providing two RLVs ($G_1 = 0.0785$ rad· μm^{-1} and $G_2 = 0.0561$ rad· μm^{-1}) and (d) a quasiperiodic DG providing three RLVs ($G_1 = 0.0785$ rad · μm^{-1}, $G_2 = 0.0561$ rad· μm^{-1} and $G_3 = 0.0436$ rad· μm^{-1}).

The experimental diffraction patterns for a periodic DG with $G_1 = 0.0785$ rad· μm^{-1} and $G_2 = 0.0561$ rad· μm^{-1} and for a QPDG are presented in figures 4(a)–(c). In figures 4(a) and (b), one can see single diffraction spots corresponding to the ±1 diffraction orders for individual periodic DGs. At the same time, the QPDG diffraction pattern contains a set of spots corresponding to the ±1 diffraction orders for both periodic DGs simultaneously. Moreover, there are additional spots in the QPDG diffraction pattern, but they are noticeably weaker.

To take into account the oblique incidence of light in the experiment, we modify the Fresnel–Kirchhoff diffraction equation as

$$U(x,y,z) = \frac{1}{i\lambda}\int\int_{-\infty}^{\infty} U(x_0,y_0,0)\frac{e^{ik\rho}}{\rho} \times e^{ik\sin(\theta)x_0}e^{-ik\sin(\theta_0)x_0}dx_0dy_0. \quad (5)$$

Here, θ_0 is the angle of incidence of light onto the grating and θ is the diffraction angle. Also the lens in the experimental setup performs the quadratic phase modulation

$$T(x,y) = e^{-ik(x^2+y^2)/2f}, \quad (6)$$

which modifies the angular scale of the image.

The experimental spatial intensity distributions for the periodic gratings with $\Lambda_1 = 80$ μm ($G_1 = 0.0785$ rad· μm^{-1}) and $\Lambda_2 = 112$ μm ($G_2 = 0.0561$ rad· μm^{-1}) are shown in figure 5(a). There are single diffraction intensity maxima corresponding to the ±1 Raman–Nath diffraction orders for

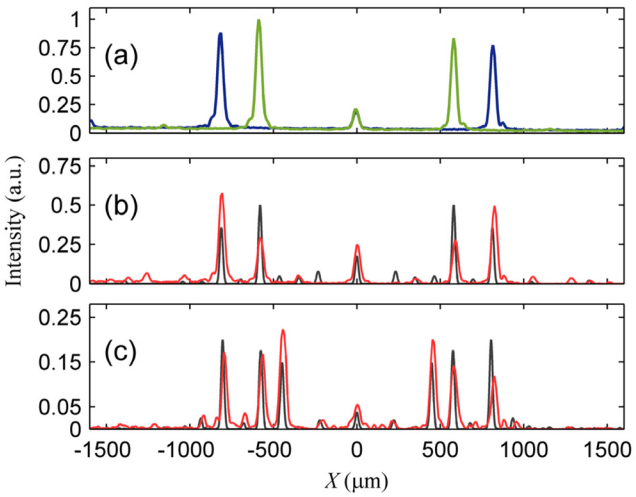

Figure 5. (a) Measured intensity distributions for a periodic DG with $\Lambda_1 = 80$ μm ($G_1 = 0.0785$ rad· μm^{-1}) (blue) and $\Lambda_2 = 112$ μm ($G_2 = 0.0561$ rad· μm^{-1})(green). (b) Measured (red) and calculated (black) intensities for a quasiperiodic DG providing two RLVs ($G_1 = 0.0785$ rad· μm^{-1} and $G_2 = 0.0561$ rad · μ m^{-1}). (c) Measured (red) and calculated (black) intensities for the quasiperiodic DG providing three RLVs ($G_1 = 0.0785$ rad· μm^{-1}, $G_2 = 0.0561$ rad · μm^{-1} and $G_3 = 0.0436$ rad· μm^{-1}).

individual periodic DGs. In figure 5(b), the measured spatial intensity distribution for the QPDG includes a set of strong maxima (± 1 Raman–Nath diffraction orders) corresponding to those for individual periodic DGs with G_1 and G_2, respectively. This can be interpreted as a splitting of the ± 1 Raman–Nath diffraction orders into several components corresponding to G_1 and G_2. Additional diffraction maxima are also observed, but they are much weaker.

The calculated intensity distribution in the QPDG diffraction pattern obtained using (5) and (6) is shown in figure 5(b). The positions of the maxima are in good agreement with the measured ones. However, one can see that the intensity distributions agree worse. In the experiment, the intensity rises from the low to high spatial frequency, while in the calculation, the situation is opposite. The calculations proved that the additional maxima correspond to the multiples of the spatial frequency $[G_1 - G_2]/2$. The maximum lying between the G_1 and G_2 maxima corresponds to the spatial frequency $[G_1 + G_2]/2$.

More than two elements in the sum in (2) can be used and, correspondingly, more than two components with different spatial frequencies will appear in the diffraction pattern. To illustrate this, figure 5(c) presents the experimental and calculated spatial intensity distributions with three components. The experimental diffraction pattern for the quasiperiodic DG providing $G_1 = 0.0785$ rad· μm^{-1}, $G_2 = 0.0561$ rad· μm^{-1} and $G_3 = 0.0436$ rad· μm^{-1} is shown in figure 4(d). Positions of the maxima are in excellent agreement, while the intensity distributions are different, as in the case of the QPDG with only two components.

Taking into account that the most of intensity is concentrated in ± 1 orders, the diffraction efficiencies for ± 1 orders in QPDG with two components are 42% for G_1, and 23% for G_2. In QPDG with three components, the first order diffraction efficiencies are 22% for G_1, 24% for G_2, and 32% for G_3.

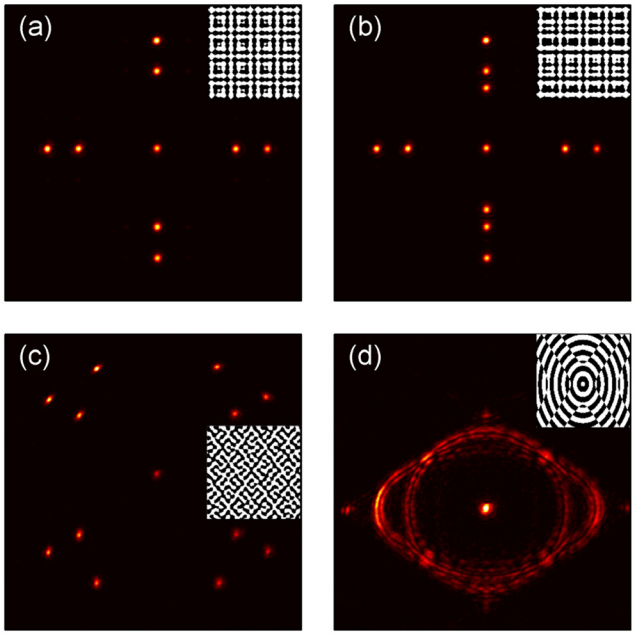

Figure 6. Experimental 2D diffraction patterns for a QPDG with the phase modulation function calculated using (7) at the $m \times n$ values of (a) 2×2 and (b) 2×3 of the corresponding phase modulation patterns (insets). (c) Experimental 2D diffraction patterns for a QPDG with the phase modulation function calculated using (8) at $m \times n - 3 \times 3$ of the corresponding phase modulation pattern (inset). (d) Experimental 2D diffraction patterns for a QPDG with the phase modulation function calculated using (2) modified for the radius vector in polar coordinates of the corresponding phase modulation pattern (inset).

The above approach can be extended to the case of the 2D intensity modulation. In this case, the phase modulation function can take the form

$$\Phi(x,y) = \Phi_0 + \Delta\Phi \cdot \mathrm{sgn}\left(\sum_{mn} a_m \cos\left[G_m^x x + \phi_m\right] + a_n \cos\left[G_n^y y + \phi_n\right]\right), \tag{7}$$

or

$$\Phi(x,y) = \Phi_0 + \Delta\Phi \cdot \mathrm{sgn}\left(\sum_{mn} a_m a_n \cos\left[G_m^x x + \phi_m\right] \cdot \cos\left[G_n^y y + \phi_n\right]\right). \tag{8}$$

The diffraction patterns for the quasiperiodic DG with the two-dimensional phase modulation are shown in figure 6. In the case described by (7), the intensity maxima are obtained if the argument of one of the cosine functions is $2\pi q$ (q is an integer), which allows us to obtain several maxima along the corresponding axis (figures 6(a) and (b)). On the contrary, the phase modulation function governed by (8) yields the intensity maxima at a specified coordinate in the $\{x, y\}$ plane (figure 6(c)). We may present (8) as modified (7) with different axes for each addend: $\Phi(x,y) = \Phi_0 + \Delta\Phi \cdot \mathrm{sgn}(\sum_{mn} a_m a_n (\cos x_{mn} + \cos y_{mn}))$, where

$x_{mn} = G_m^x x + G_n^y y$ and $y_{mn} = G_m^x x - G_n^y y$. Thus, in the case described by (8), the intensity maxima are obtained at the coordinates $\{\pm x, \pm\frac{G_m^x}{G_n^y}x\}$. The proposed approach can be used to form not only discrete, but also continuous diffraction. For instance, if we substitute x in the (2) with the radius vector r as $\Phi(r) = \Phi_0 + \Delta\Phi \cdot \mathrm{sgn}(\sum_{mn} a_{mn} \cos(r)$, where $r = \sqrt{(G_m^x x)^2 + (G_n^y y)^2}$; thus we will be able to obtain continuous ring-shaped diffraction patterns (figure 6(d)). Since the SLM has a finite pixel size, it cannot generate perfectly circular patterns; therefore, this ring-shaped diffraction patterns will most likely be somewhat distorted. In the experiment, we used the RLV values of $G_1^x = G_1^y = 0.0785\,\mathrm{rad}\cdot\mu\mathrm{m}^{-1}$, $G_2^x = G_2^y = 0.0561\,\mathrm{rad}\cdot\mu\mathrm{m}^{-1}$, and $G_3^x = G_3^y = 0.0436\,\mathrm{rad}\cdot\mu\mathrm{m}^{-1}$.

Since such QPDGs can be created not only by the SLM, but also by other methods, e.g. mechanical and photolithographic ones, the limitations imposed on the reciprocal lattice vectors by the SLM pixel size can be eliminated. In addition, the intensity distribution over all the maxima can be tailored by varying the amplitudes a_n in (2). In practice, the Bragg diffraction mode is preferred (beneficial) because of its highest efficiency. The approach proposed can also be used to structure a diffraction grating operating in the Bragg mode.

4. Conclusion

In conclusion, we elaborated and experimentally proved the analytical method, which makes it possible to form a discrete diffraction pattern consisting of a set of fixed-order diffraction maxima using a quasiperiodic diffraction grating. This analytical approach allows one to control a number of diffraction maxima, intensity distribution between them, and their angular positions by choosing appropriate reciprocal lattice vectors and their amplitudes. This analytical method is applicable to both one- and two-dimensional quasiperiodic gratings. Moreover, using quasiperiodic diffraction gratings, several diffraction maxima with different wavelengths and propagation directions can be coupled in a single diffraction maximum.

Acknowledgments

The authors thank Prof Anatoly S Chirkin and Sergey A Myslivets for help and fruitful discussions.

References

[1] Bonod N and Neauport J 2016 Diffraction gratings: from principles to applications in high-intensity lasers *Adv. Opt. Photon.* **8** 156–99
[2] Doskolovich L L, Kharitonov S I, Petrova O I and Soifer V A 1998 A gradient method for design of multiorder varied-depth binary diffraction gratings *Opt. Laser Eng.* **29** 249–59
[3] Albero J, Moreno I, Davis J A, Cottrell D M and Sand D 2012 Generalized phase diffraction gratings with tailored intensity *Opt. Lett.* **37** 4227–9
[4] Gao N and Xie C 2011 High-order diffraction suppression using modulated groove position gratings *Opt. Lett.* **36** 4251–3
[5] Sanchez-Brea L M, Jose Torcal-Milla F and Buencuerpo J 2018 Far-field diffraction of linear chirped gratings *Opt. Laser Technol.* **107** 337–43
[6] Gao N, Li H, Zhu X, Hua Y and Xie C 2013 Quasi-periodic gratings: diffraction orders accelerate along curves *Opt. Lett.* **38** 2829–31
[7] Verma R, Sharma M K, Senthilkumaran P and Banerjee V 2014 Analysis of Fibonacci gratings and their diffraction patterns *J. Opt. Soc. Am.* A **31** 1473–80
[8] Wu K and Wang G P 2013 One-dimensional Fibonacci grating for far-field super-resolution imaging *Opt. Lett.* **38** 2032–4
[9] Ferrando V, Giménez F, Furlan W D and Monsoriu J A 2015 Bifractal focusing and imaging properties of Thue–Morse Zone Plates *Opt. Express* **23** 19846–53
[10] Saavedra G, Furlan W D and Monsoriu J A 2003 Fractal zone plates *Opt. Lett.* **28** 971–3
[11] Brown B R and Lohmann A W 1969 Computer-generated binary holograms *IBM J. Res. Dev.* **13** 160
[12] Suh H H, Kwak C H and Lee E-H 1995 Combined binary-phase holograms for free-space optical interconnection *Opt. Lett.* **20** 2131–3
[13] Lohmann A W, Schwider J, Streibl N and Thomas J 1988 Array illuminator based on phase contrast *Appl. Opt.* **27** 2915–21
[14] Vasara A, Taghizadeh M R, Turunen J, Westerholm J, Noponen E, Ichikawa H, Michael Miller J, Jaakkola T and Kuisma S 1992 Binary surface-relief gratings for array illumination in digital optics *Appl. Opt.* **31** 3320–36
[15] Shapira A, Juwiler I and Arie A 2011 Nonlinear computer-generated holograms *Opt. Lett.* **36** 3015–7
[16] Leshem A, Shiloh R and Arie A 2014 Experimental realization of spectral shaping using nonlinear optical holograms *Opt. Lett.* **39** 5370–3
[17] Lee W-H 1979 High efficiency multiple beam gratings *Appl. Opt.* **18** 2152–8
[18] Ren T W, He J L, Zhang C, Zhu S N, Zhu Y Y and Hang Y 2004 Simultaneous generation of three primary colours using aperiodically poled $LiTaO_3$ *J. Phys.: Condens. Matter* **16** 3289
[19] Novikov A A and Chirkin A S 2008 Coupled multiwave interactions in aperiodically poled nonlinear optical crystals *J. Exp. Theor. Phys.* **106** 415
[20] Chirkin A S and Shutov I V 2008 Parametric amplification of light waves at low-frequency pumping in aperiodic nonlinear photonic crystals *J. Exp. Theor. Phys. Lett.* **86** 693
[21] Chirkin A S and Shutov I V 2009 Parametric amplification of light waves at low-frequency pumping in aperiodic nonlinear photonic crystals *J. Exp. Theor. Phys.* **109** 547
[22] Vyunishev A M and Chirkin A S 2015 Multiple quasi-phase-matching in nonlinear Raman-Nath diffraction *Opt. Lett.* **40** 1314
[23] Vyunishev A M, Pankin P S, Svyakhovskiy S E, Timofeev I V and Ya Vetrov S 2017 Quasiperiodic one-dimensional photonic crystals with adjustable multiple photonic bandgaps *Opt. Lett.* **42** 3602–5